Direct Electrostatic Calibration of Hybrid Sensors for Small Force Measurement

Koo-Hyun Chung, Gordon A. Shaw, and Jon R. Pratt

Manufacturing Engineering Laboratory, National Institute of Standards and Technology,

100 Bureau Drive, Stop 8221, Gaithersburg, Maryland 20899

ABSTRACT

The measurement of forces from piconewtons to millinewtons is an area of interest from both an applied and pure research standpoint. However, creating a link between small forces and the International System of Units (SI) has been difficult. In this work, a hybrid sensor was examined using small force measurement techniques. SI-traceable forces were applied to the sensor using two methods, one yielding a compressive and the other a tensile load. Compressive loads were realized using an auxiliary force cell previously calibrated using deadweights. Tensile loads were realized in a new fashion by creating a calculable electrostatic force between a spherical electrode on the hybrid sensor load button and a fixed, flat electrode located in close proximity to the sphere. Each of the loading conditions caused measurable deflections of the hybrid sensor load button, which were recorded using the sensor's on-board displacement metrology. The applied loads and measured deflections were used to calculate the spring constant of the sensor. Results obtained for the computed spring constant were consistent for both loading schemes, suggesting the new electrostatic loading scheme is a viable alternative to the more traditional force cell approach.

1. INTRODUCTION

Recently, nano-scale mechanical test instruments such as instrumented indenters and atomic force microscopes (AFM) have been widely utilized for characterization of various properties. The measurements of small forces by AFM as well as by nano-indentation techniques have been increasing in the mechanical analysis of thin films [1] and biological materials such as collagen fibrils [2] and DNA [3]. Furthermore, to gain a better understanding of the nano-mechanical properties, extensive efforts have been made to extend displacement and force resolution to nanometer and nanonewton levels. However, maintaining a traceable pathway for small force calibrations in the regime of micronewtons and below is difficult due to uncertainties that accrue with transferring measurements of force obtained from traceable deadweights [4]. As an effort to overcome this, a primary reference device, the electrostatic force balance (EFB), has been created to realize electrostatic forces in the International System of Units (SI)-traceable fashion [4,5]. One of the applications of the EFB is the calibration of AFM cantilever spring constants [6,7], in which a traceably calibrated cantilever spring constant can aid in the use of AFM for quantitative force measurement and to verify the accuracy of other calibration procedures [8].

In a fashion similar to AFM, instrumented indenters often employ an internal spring as a reference standard for small force measurement. The indenter has been often used as a reference spring for spring constant calibration of force sensors [9,10]. For accurate small force measurement, this spring must be calibrated in a traceable fashion. Towards this end, we propose a new SI-traceable electrostatic method for realizing small forces that can be employed to apply tensile forces directly to instrumented indentation sensors, provided that their load button can accommodate the attachment of a small spherical electrode. As a proof of concept, we attempt to determine the spring constant of a hybrid small force sensor using our new loading technique. With this value in hand, the measurement is repeated substituting a deadweight-calibrated auxiliary force transducer as the source of the calibration force. The two independent small force measurement techniques provide an opportunity to reveal potential systematic discrepancies between the procedures, most particularly if there is any dependence of the hybrid sensor calibration on the direction of loading. The following sections describe the experimental details and results.

2. EXPERIMENTAL DETAILS

The schematic of the hybrid sensor head is given in Figure 1. The sensor head was designed for instrumented indentation and is an "add-on" attachment to our general purpose laboratory AFM. The displacement of the sensor head with respect to the sample was controlled using the fine motion piezo-actuated scanner of the AFM. This z-scanner has a linear variable displacement transformer (LVDT) to record its extension, and we employed this signal to perform closed-loop feedback control of the scanner displacement during the experiments. According to the manufacturer's product literature, the sensor head consists of a uni-axial flexure which deflects

as the load button/indenter tip is pressed into a surface by the z-scanner. The deflection of this flexure spring with respect to the displaced body of the z-scanner is measured using an optical lever arm sensor (essentially an AFM detection scheme) mounted above the flexure spring and fixed to the body of the sensor head, which is rigidly attached to the z-scanner. To convert the deflection of the flexure to force, it is necessary to know the spring constant of the flexure mechanism.

The calibration process was divided into two steps. First, the sensitivity of the optical lever arm to flexure deflection was calibrated, and then deflection in response to known forces was measured. As shown in Figure 1, a steel ball bearing with a radius of about 1 mm was glued to a screw that was compatible with the sensor's holder. For electrical connection, a coaxial cable was soldered to the side of the steel ball. A very thin cable was used to minimize the influence of the cable on the flexure spring.
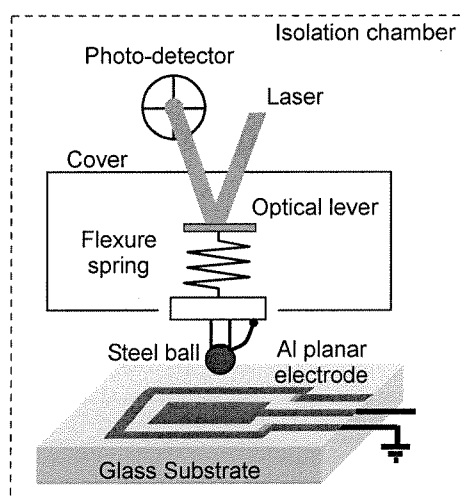

Figure 1. Schematic of the hybrid sensor and experimental scheme for traceable electrostatic force calibration.

After the adjustment of the photodiode and superluminescent diode (SLD) used in the optical lever arm detector, three hours of equilibration were allowed in an isolation chamber. The sensitivity of the optical lever with respect to the displacement was then calibrated by pressing the steel ball indenter tip against a rigid surface ten times. The sensitivity of the optical lever arm was calibrated by fitting a straight line to the photodiode voltage vs. indenter displacement curve. In this fashion, a traceable pathway is established for the determination of the flexure displacement by the comparison to the LVDT displacement, which was compared to the output of a laser interferometer by the AFM manufacturer and makes the necessary link to an SI realization of length based on the wavelength of light. Errors, such as cosine and Abbé, induced by the lack of coincidence between the indenter and LVDT axes are assumed negligible, and we assume that the relative standard uncertainty of the applied displacement is better than 10^{-2} for the range of displacements encountered here. The measurement was repeated four times. The photodiode as well as SLD were re-adjusted before each repetition. The mean sensitivity S was 2.26×10^{-3} V/nm and the standard deviation $u(S_i)$ of the four determinations was 1.2×10^{-4}.

The auxiliary force transducer used to apply compressive forces to the indenter was calibrated using traceable deadweights which were placed on the transducer using an automated system [11]. The force read-out of this transducer is measured in capacitance, which we recorded using an ultra-precision capacitance bridge (Andeen-Hagerling) as deadweight forces were applied to the load button in increments ranging from 50 µN to 5000 µN. Each of the deadweight force increments were applied ten times. The transducer was unloaded between each weighing so the drift in capacitance could be subtracted. The relationship between corrected capacitance and deadweight was obtained from a cubic polynomial fit. The calibrations were performed for two force regimes to improve the accuracy of the curve fitting: the high range encompassed forces from 500 µN to 5000 µN and the low range, 50 µN to 500 µN.

After placing the auxiliary force transducer beneath the indentation sensor, the system was allowed to equilibrate for several hours in the isolation chamber. A displacement-controlled indentation experiment was then performed. Five linearly increasing positions were sampled, with a return to the initial out-of-contact location between each position in order to monitor and subtract the drift from the final measurement. Ten measurements of the force transducer capacitance, indenter position, and photodiode voltage were acquired for each step. Each measurement was repeated four times. The indenter spring constant was obtained by converting the capacitance change from each loading position into force (F), and displacement (x) was determined by using initially measured sensitivities of the optical lever arm. This allowed the calculation of the flexure spring constant, k, from Hooke's law:

$$F = kx \qquad (1)$$

Next, an electrostatic force-based calibration of the indenter spring constant was attempted. The procedure involved the direct application of an electrostatic force between a spherical metal electrode attached to the hybrid sensor and a planar thin film electrode. The application of a voltage between the tip and planar electrode results in a net attractive force on the sphere applied through the center of the sphere to the point closest to the planar electrode surface such that

$$F = \frac{1}{2} \frac{dC}{dz} V^2 \qquad (2)$$

where C is capacitance, z is position, and V is applied voltage. The force in Eq. (2) was calculated using traceable evaluations of V, C, and z. A thin-film planar aluminum electrode with approximate dimensions of 2 cm by 2 cm was used as the fixed electrode which was located under the steel ball mounted on the sensor. The fixed electrode was surrounded by a grounded guard ring to minimize stray capacitance. Three terminal capacitance values were measured using an Andeen-Hagerling (AH) capacitance bridge. Capacitance transfer using this bridge is estimated to have a relative standard uncertainty $u(C_i)/|C_i|$ of 3×10^{-6} based on manufacturer's data. Fixed bias voltages up to 100 V were applied through the capacitance bridge. The applied bias voltage

was measured using an Agilent 3458a voltmeter that was recently calibrated against Zener and resistive divider standards at NIST that are traceable to an SI realization of the volt achieved using a Josephson junction array. Relative standard uncertainty $u(V_i)/|V_i|$ of voltage transfer on this scale is conservatively estimated at 1×10^{-5}. Once again, the z-position traceability is established through transfer from the factory-calibrated LVDT.

To determine the capacitance gradient (dC/dz), the position of the z-scanner was varied using feedback control based on the LVDT position sensor readout. The sensor head was positioned approximately in the center of the z scan range over which the capacitance gradient was determined. The function $C(z)$ was mapped by commanding z positions in descending fixed steps that progressively brought the sphere closer to the fixed electrode. Each step towards the surface was followed by a return to a predefined home position, to provide a measure of the drift during the measurements.

Finally, stepwise voltages were applied with five increments. The measurement was repeated ten times. The individual values of dC/dz obtained before and after applying voltage were averaged to correct for drift and the average was used to determine each spring constant. It should be noted that the initially-determined value of optical lever arm sensitivity (2.33×10^{-3} V/nm) was used for all measurements. Since the maximum bias that could be applied to the AH capacitance bridge was 100 V, it was necessary to work at very small indenter-fixed electrode separations, typically less than approximately 500 nm, in order to achieve gradients that produced measurable forces at these voltages. Flexure deflection in response to the electrostatic force was determined using the optical lever signal. Capacitance gradients were interleaved with the application of voltages.

3. RESULTS AND DISCUSSION

Representative results from the spring constant calibration using the force transducer are shown in Figure 2. A high degree of linearity can be observed for both the high- and low- load cases and the relative residuals of the curve fits were less than 1%. The obtained spring constant k_h of the indenter was 3944 N/m and the standard deviation $u(k_{h,i})$ was 214 N/m (5.4 % relative standard deviation) for the high force range, and the obtained spring constant k_l was 3926 N/m with a standard deviation $u(k_{l,i})$ of 209 N/m (5.3 % relative standard deviation) for the low force range. The difference between those values, $(k_h - k_l)/k_l$, was 4.6×10^{-3}, which was within the statistical uncertainties of calibration. The sources of uncertainty and the magnitudes are summarized in Table 1. The combined relative standard uncertainty u_c [12] of the calibration was 5.28×10^{-2}. It was concluded that the uncertainty of the indenter calibration was mainly due to the uncertainty of optical lever calibration. Because the optical lever arm was readjusted between trials, we expect this uncertainty could be significantly reduced by employing better procedures for adjusting the optical lever during calibration.
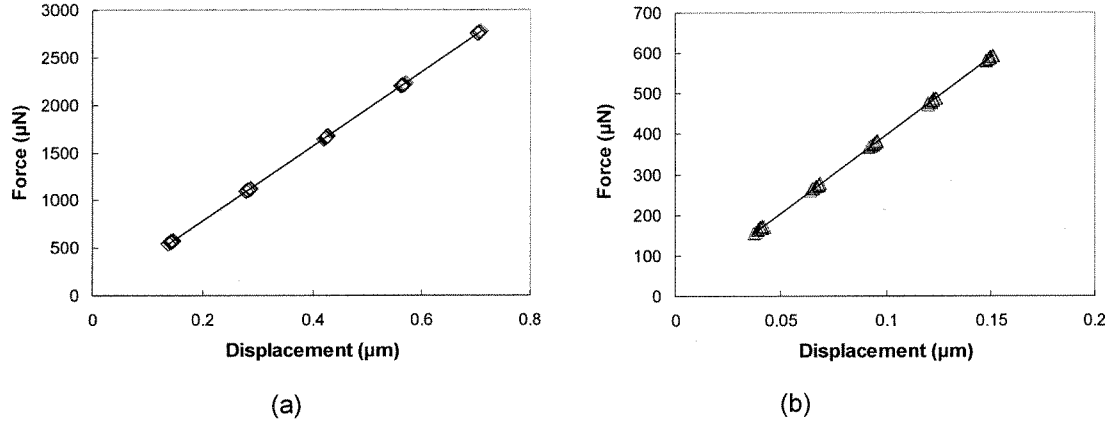
Figure 2. Representative spring constant calibration of indenter using force transducer (a) for high force range and (b) low force range.

Table 1. Uncertainty (type A) in spring constant calibration using the auxiliary force transducer.

Source	Magnitude of relative standard uncertainty
Calibration of optical lever arm sensitivity	5.27×10^{-2}
Measurement of optical lever signal	1.4×10^{-3}
Calibrated force transducer	3.0×10^{-3}
Combined standard uncertainty	5.28×10^{-2}

A representative result obtained for the measurement of the function $C(z)$ is shown in Figure 3 (a). Based on the data shown in this plot, the function appears to be linear over the displacement range, and the capacitance gradient was approximated using a least squares best fit straight line. The mean gradient based on ten such curve fits was 39.72 pf/mm with a standard uncertainty of 0.67 pf/mm.

Finally, a representative result from the spring constant calibration using electrostatic forces to apply tensile loads is shown in Figure 3 (b). Due to the constraint on applied voltage, the maximum tensile force was approximately 150 μN. As a result, position changes of less than 50 nm were typical. Ten experiments were carried out, and the average spring constant from the electrostatic calibration, k_e, was 3759 N/m ± 153 N/m (4.1 % relative standard deviation). The difference between the spring constants from the electrostatic (tensile loading) calibration and the auxiliary force transducer calibration (for compressive loads less than 500 μN) is $(k_l - k_e)/k_e = 4.4 \times 10^{-2}$. It is believed that the difference in the optical lever arm sensitivity used in the two calibration methods resulted in the difference between the computed spring constants. Table 2 shows the sources of uncertainties and their magnitudes for the spring constant calibration based on the electrostatic force. A rigorous uncertainty analysis for the electrostatic calibration is in process and will be reported in future work. In contrast to the experiment with the auxiliary force transducer, the uncertainty in the optical lever arm sensitivity was not considered in this experiment.
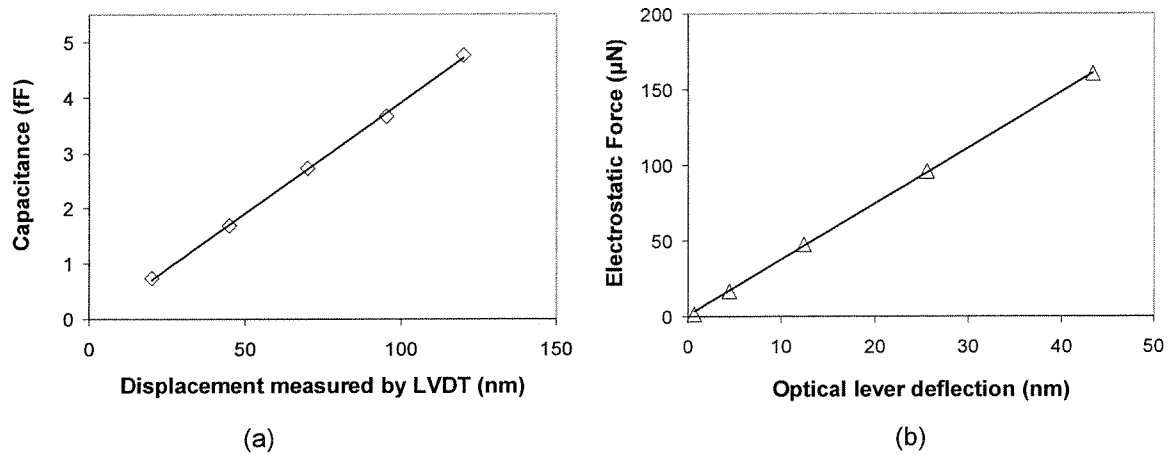
Figure 3. (a) Capacitance gradient of indenter system for small tip sample separations and (b) an electrostatic indenter spring constant calibration.

Table 2. Uncertainty (type A) in spring constant calibration using electrostatic force.

Source	Magnitude of relative standard uncertainty
Measurement of optical lever signal	2.93×10^{-2}
Measurement of applied voltage	2×10^{-4}
dC/dz	1.70×10^{-2}
Combined standard uncertainty	3.39×10^{-2}

4.   Conclusions

The spring constant of an instrumented indentation sensor was measured using SI-traceable force metrology at the NIST small force measurement laboratory.   The indenter was first calibrated by using an SI-traceable auxiliary force transducer.   Proper technique allowed the determination of the indenter spring constant with percent-level repeatability.   The spring constants obtained by applying compressive stress for high and low force ranges was 3944 N/m ± 214 N/m and 3926 N/m ± 209 N/m, respectively.   It was found that the most significant source of uncertainty in both force ranges was the optical lever sensitivity calibration.   Also, a novel electrostatic method for indenter force calibration was developed and the spring constant of 3759 N/m ± 153 N/m was obtained. The results showed that the difference between the spring constants from the electrostatic (tensile loading) calibration and the auxiliary force transducer calibration (for compressive loads less than 500 μN) is $(k_l - k_e)/k_e = 4.4 \times 10^{-2}$, which was within experimental uncertainty.

Acknowledgement

Disclaimer

References

1. VanLandingham M. R., Review of instrumented indentation, *J Res. Natl. Inst. Stand. Technol.*, 108, 249-265, 2003.

2. McDaniel D. P., Shaw G. A., Elliott J. T., Bhadriraju K., Meuse C., Chung K. H., and Plant, A. L., The stiffness of collagen fibrils influences vascular smooth muscle cell phenotype, *Biophys J.*, 92, 1759-1769, 2007.

3. Smith, S.B., Cui Y., Bustamante C., Overstretching B-DNA, *Science*, 271, 795-799, 1996.

4. Pratt, J. R., Newell, D. B., Kramar, J. A., and Smith, D. T., Review of SI traceable force metrology for instrumented indentation and atomic force microscopy, *Meas. Sci. Technol.*, 16, 2129-2137, 2005

5. Pratt, J. R., Smith, D. T., Newell, D. B., Kramar, J. A., and Whitenton E., Progress toward Système International d'Unités traceable force metrology for nanomechanics, *J. Mater. Res.*, 19, 366-379, 2004.

6. Shaw, G. A., Kramar, J. A., and J. R. Pratt, SI-traceable spring constant calibration of microfabricated cantilevers for small force measurement, *Exp. Mech.*, 47, 143-151, 2007.

7. Gates, R. S. and Pratt, J. R., Prototype cantilevers for SI-traceable nanonewton force calibration, *Meas. Sci. Technol.*, 17, 2852-2850, 2006.

8. Matei, G. A., Thoreson, E. J., Pratt, J. R., Newell, D. B., and Burnham, N. A., Precision and accuracy of thermal calibration of atomic force microscopy cantilevers, *Rev.Sci. Inst.*, 77, 0837031-6, 2006.

9. Holbery J. D., Eden V. L., A comparison of scanning microscopy cantilever spring force constants determined using a nanoindentation testing apparatus, *J Micromech. Microeng.*, 10, 85-92, 2005.

10. Syed Asif S. A., Whal, K. J., and Colton R. J., Nanoindentation and contact stiffness measurement using force modulation with a capacitive load-displacement transducer, *Rev. Sci. Instrum.*, 70, 2408-2413. 2413.

11. Seugling, N. A., Pratt J. R., Traceable force metrology for micronewton level calibration, *Proc. ASPE*, Annual Meeting, Orlando, FL, 2004.

12. Taylor, B. N. and Kuyatt, C. C., Guidelines for evaluating and expressing the uncertainty of NIST measurement results, *NIST technical note*, 1297, 1994.

SEM

Proceedings of the 2007 SEM Annual Conference and Exposition on Experimental and Applied Mechanics

June 4-6, 2007
Springfield, Massachusetts USA